

Northumbria Research Link

Citation: Mendes, Joao, Gallipoli, D., Boeck, F. and Tarantino, A. (2020) A comparative study of high capacity tensiometer designs. *Physics and Chemistry of the Earth, Parts A/B/C*, 120. p. 102901. ISSN 1474-7065

Published by: Elsevier

URL: <https://doi.org/10.1016/j.pce.2020.102901>
<<https://doi.org/10.1016/j.pce.2020.102901>>

This version was downloaded from Northumbria Research Link:
<http://nrl.northumbria.ac.uk/id/eprint/44200/>

Northumbria University has developed Northumbria Research Link (NRL) to enable users to access the University's research output. Copyright © and moral rights for items on NRL are retained by the individual author(s) and/or other copyright owners. Single copies of full items can be reproduced, displayed or performed, and given to third parties in any format or medium for personal research or study, educational, or not-for-profit purposes without prior permission or charge, provided the authors, title and full bibliographic details are given, as well as a hyperlink and/or URL to the original metadata page. The content must not be changed in any way. Full items must not be sold commercially in any format or medium without formal permission of the copyright holder. The full policy is available online: <http://nrl.northumbria.ac.uk/policies.html>

This document may differ from the final, published version of the research and has been made available online in accordance with publisher policies. To read and/or cite from the published version of the research, please visit the publisher's website (a subscription may be required.)

1

Title:	A comparative study of designs of high capacity tensiometers
Revision	R1
Keywords:	High capacity tensiometers, soil suction, laboratory testing

2

3

4

	Author	Affiliation	Email Address
1	Joao Mendes*	Department of Mechanical & Construction Engineering, Northumbria University, United Kingdom	joao.mendes@northumbria.ac.uk
2	Domenico Gallipoli	Dipartimento di Ingegneria civile, chimica e ambientale (DICCA), Università degli Studi di Genova , Italy Formerly Laboratoire SIAME, Fédération IPRA, Université de Pau et des Pays de l'Adour, France	domenico.gallipoli@unige.it
3	Flora Boeck	Formerly UMS - METER Group AG, Germany	floralisaboeck@gmail.com
4	Alessandro Tarantino	Department of Civil and Environmental Engineering, University of Strathclyde, United Kingdom	alessandro.tarantino@strath.ac.uk

5

6 * - **Corresponding author:**

7 **Address:**

8 Northumbria University

9 Faculty of Engineering and Environment

10 Department of Mechanical & Construction Engineering

11 Wynne Jones Building, Room 117

12 Newcastle upon Tyne, NE1 8ST

13 United Kingdom

14

15 **E-mail:**

16 joao.mendes@northumbria.ac.uk

1 **Highlights:**

2

3 • *The suction measuring range of seven distinct high capacity tensiometer prototypes has been*
4 *compared*

5

6 • *Larger air entry value of the porous filter increases the suction measurement range*

7

8 • *The air entry value is inversely related to the size of largest pore in the porous filter*

9

10 • *Water reservoir size and protective casing have little influence on the suction range*

11

12 • *The application of larger water pressures during saturation increases the suction range*

13

14

15

1 A comparative study of High Capacity Tensiometer 2 designs

3

4 **Mendes J., Gallipoli D., Boeck F., Tarantino A.**

5

6 **Abstract**

7 The High Capacity Tensiometer (HCT) is a soil sensor that can measure large negative pore-water
8 pressures, i.e. in excess of -1 MPa, and is a key instrument for monitoring ground-atmosphere interactions.
9 The design of HCTs has not changed since the first prototype was proposed in the 1990s and still includes
10 three main components, namely a high air-entry value porous filter, a small water reservoir and a pressure
11 transducer, which are all encased inside a protective sheath. Despite many successful examples of
12 measurement of pore-water tension in the laboratory and the field, there are essentially no commercially
13 available HCTs for industrial applications. The rare utilisation of HCTs in engineering practice has always
14 relied on bespoke devices that have been purposely designed by research laboratories or suppliers of soil
15 sensors. The dissemination of HCTs into engineering practice has been further hindered by the relatively
16 poor understanding of sensor design and its impact on the reliability of measurements. To overcome such
17 gap of knowledge, this paper explores the influence of distinct design variables (i.e. the porous filter, the
18 pressure transducer, the water reservoir size and the protective casing) on the measuring range of HCTs.
19 Seven prototypes were manufactured with different combinations of the above design variables showing
20 that, if HCTs are properly saturated, the air entry value of the filter has the strongest influence on the
21 measuring range while the effects of reservoir size, pressure transducer and protective casing are relatively
22 modest. It is expected that the results from this work will guide future design of HCTs, thus contributing to
23 the development of resilient sensors for geotechnical applications.

24

25 **Keywords**

26 High capacity tensiometers, pore-water tension, soil suction.

1 Introduction

2 Natural soils and geotechnical infrastructure (e.g. road/railway/flood embankments and earth dams) are
3 strongly affected by evapotranspiration and the consequent occurrence of capillary (tensile) water close to
4 the ground surface. In the vadose region, pore-water pressures are negative and soil suction is defined as
5 the difference between pore-air and pore-water pressure which means that, under atmospheric conditions,
6 soil suction coincides with the negative pore-water pressure changed of sign.

7 A number of instruments are commercially available to measure negative pore-water pressures in soils and,
8 among these, the most common options are conventional tensiometers and porous block sensors. Conventional
9 tensiometers provide a direct measurement of negative pore-water pressures over a relatively
10 limited range of values, from 0 to -80 kPa, which is often exceeded in the field especially during dry spells.
11 Instead, porous block sensors provide an indirect record of negative pore-water pressures based on the
12 measurement of the electrical or thermal properties of a porous element in contact with the soil. Porous
13 block sensors are generally unsuitable for geotechnical applications as they suffer from a slow response
14 time and poor accuracy. For example, they are unable to capture the rapid changes of soil suction caused
15 by the fast propagation of a water front during rainwater infiltration.

16 In contrast with commercial devices, the High Capacity Tensiometer (HCT) is a sensor that can measure
17 large pore-water tensions, well beyond the water cavitation threshold of -100 kPa, with a relatively quick
18 response and good accuracy. The first HCT prototype was developed by Ridley and Burland (1993) and
19 measured negative pore-water pressures in excess of -1500 kPa. This pioneering work provided the basis
20 for the subsequent design of a number of HCT prototypes by different research groups around the world
21 (Guan and Fredlund, 1997; Marinho and de Sousa Pinto, 1997; Tarantino and Mongiovi, 2002; Meilani
22 et al., 2002; Take and Bolton, 2003; Toker et al., 2004; Lourenco et al., 2008; Cui et al., 2008; Mendes and
23 Buzzi, 2014; Bagheri et al., 2018). The reader may refer to Marinho et al. (2008) for a review of the
24 theoretical and practical aspects of suction measurement by means of HCTs.

25 To date, HCTs have been used in the field to monitor pore-water pressures inside slopes or agricultural
26 soils (Mendes et al., 2008, Cui et al. 2008, Toll et al. 2011) but also in the laboratory to measure the changes
27 of suction during oedometer tests (Tarantino and De Col 2008; Le et al. 2011; Wijaya and Leong, 2016),
28 direct shear tests (Caruso and Tarantino, 2004) and triaxial tests (Cunningham et al. 2003; Mendes and
29 Toll, 2016). Past studies have always made use of bespoke devices that have been purposely designed and
30 manufactured by research laboratories and suppliers of soil sensors. Two main concept of HCT design have
31 been put forward over the years: in one case, the HCT incorporates a strain gauge pressure transducer that
32 forms an integral part of the sensor body (Tarantino and Mongiovi, 2002) while, in the other case, the HCT
33 consists of the assembly of a commercial pressure transducer and a porous filter, which are glued with an
34 epoxy resin inside a protective casing (Delage et al., 2008). The former design concept has the advantage
35 of minimizing the number of connections between parts and therefore reduces the potential entrapment of
36 air cavitation nuclei. This design is however difficult to manufacture and suffers from high temperature
37 sensitivity, which makes it unsuitable for field use. The latter design concept overcomes these limitations
38 while preserving a good measuring performance (Delage et al., 2008) and is therefore the preferred choice
39 for industrial applications.

40 In spite of many successful examples of suction measurement in the laboratory and in the field, there are
41 no commercially available HCTs for routine engineering applications. The dissemination of HCTs beyond
42 the academic context has also been impeded by a relatively poor understanding of sensor design in relation
43 to measuring performance. To overcome this limitation, the present paper investigates the measuring range
44 of seven different HCT prototypes manufactured according to the latter of the above two design concepts.
45 The study analyses different combinations of porous filters, pressure transducers, water reservoir sizes and
46 protective casings to identify their effect on the sensor measuring range. The procedures for saturating
47 HCTs are also briefly discussed in the paper. The objective is to highlight the advantages and disadvantages
48 of different prototypes in order to support the future design of HCTs that may attract the interest of
49 geotechnical practitioners.

2 Background

Figure 1 shows the first HCT developed in the 1990s at the Imperial College, London, by Ridley and Burland (1993). Since then, the design of HCTs has changed relatively little and it still comprises the following three main components: a) a high air entry value porous filter which is typically made of ceramic, b) a small water reservoir with a capacity between 10 mm³ and 100 mm³ and c) a pressure transducer, which may consist of either an integral strain gauge diaphragm or an off-the-shelf commercial device.

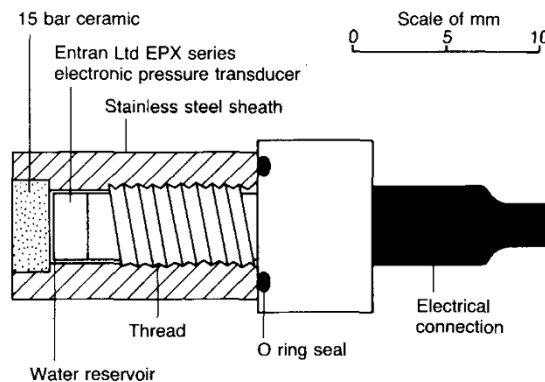


Figure 1. Imperial College HCT (Ridley and Burland, 1993).

After saturation of the HCT with water, the outer face of the porous filter is placed in contact with the soil whose suction will be measured. The porous filter has therefore the purpose of ensuring the hydraulic continuity between the water inside the HCT reservoir and the soil. Mendes et al. (2015) suggested that, among all design components, the porous filter has the strongest influence on the maximum water tension that can be sustained by the HCT (i.e. the measuring range of the HCT). Indeed, the Air Entry Value (AEV) of the porous filter often coincides with the maximum water tension that a HCT can measure. For example, this is the case for the HCT shown in Figure 1 which, according to Ridley and Burland (1993), measured a maximum pore-water tension of about -1500 kPa that is consistent with the 15 bar AEV of the ceramic filter. This would imply that, if the ceramic filter is in contact with a saturated clay having an air-entry suction greater than the AEV of the filter, the maximum suction measured by the tensiometer would coincide with the air-entry suction of the clay rather than the AEV of the filter. Nevertheless, this aspect has never been investigated experimentally in detail.

The purpose of the water reservoir is to allow the small inwards deflection of the transducer diaphragm during suction measurements. Past evidence suggests that the size of the water reservoir does not influence the measuring range of the sensor (Mendes and Buzzi, 2013), though a large reservoir might undermine the long-term stability of measurements (Mendes and Gallipoli, 2020).

The external casing protects the filter, the pressure transducer and the water reservoir from the application of external loads, which could generate additional deformations of the sensing diaphragm and, hence, produce spurious measurements of water pressure. External loads may be caused by mechanical actions during installation and measurement but also by the different thermal expansion/contraction of the casing and pressure transducer. These effects cannot be accounted for by zeroing the readings before installation with the HCT under stress-free conditions and at a constant ambient temperature, because these conditions differ from those inside the ground. Particular care should therefore be taken when choosing the material and the geometry of the protective casing so as to minimize the occurrence of spurious measurements. Reading inaccuracies are more likely to occur if the sensing diaphragm is an integral part of the sensor body.

Finally, adequate procedures should be adopted to minimise the air trapped inside the reservoir and filter during saturation of HCTs because the presence of gas nuclei may induce errors in measurements, reduce

1 the maximum sustainable suction and undermine the stability of readings over time (Mendes and Gallipoli,
2 2020).

3 **3 Design of HCT prototypes**

4 The seven prototypes investigated in the present work were designed and manufactured with: a) two
5 different ceramic filters presenting distinct mineralogical compositions and pore size distributions, b) two
6 different pressure transducers with distinct geometries, i.e. a flush diaphragm transducer and a cavity
7 diaphragm transducer, c) two different water reservoir sizes (corresponding to the different pressure
8 transducer geometries) and d) two different protective casings made of stainless steel and ceramic.

9

10 **3.1 Ceramic filters**

11 Among all design components, the AEV of the filter has the strongest influence on the maximum water
12 tension that can be sustained by HCTs. The AEV is the maximum difference that can exist between the air
13 and water pressures acting on the two sides of a saturated filter (with the former being larger than the latter)
14 without allowing the air to break through the filter. During field measurements, the air pressure on the
15 external face of the HCT filter is atmospheric while the water inside the reservoir is under tension. Note
16 that this is unlike the measurement of the AEV in the laboratory where the air pressure on one side of the
17 saturated filter is usually bigger than atmospheric while the water pressure on the other side is atmospheric.

18 The above pressure difference can be sustained by the saturated filter thanks to the formation of concave
19 water menisci on the side of the filter that is exposed to the air. These menisci act as a “membrane”, which
20 separates the air from the water up until the attainment of the maximum possible pressure difference, i.e.
21 the AEV of the filter. Once this limit is exceeded, the air penetrates inside the filter as a separate phase
22 causing the desaturation of the HCT and the consequent breakdown of suction measurements. The AEV of
23 the filter therefore constitutes an upper bound of the maximum suction that can be measured by HCTs.

24 The AEV is inversely related to the size of the largest pore inside the filter, which means that smaller pore
25 sizes correspond to greater AEVs and therefore to greater maximum sustainable water tensions. This is also
26 consistent with the predictions of the Young-Laplace equation which, under the simplifying hypothesis of
27 cylindrical pores, shows that the AEV is inversely proportional to the largest pore diameter, d_{max} :

$$28 \quad AEV = \frac{4 \sigma_w \cos \theta_w}{d_{max}} \quad [1]$$

29 where, σ_w is the air-water surface tension (72.8 mN/m at 293 °K) and θ_w is the contact angle between the
30 filter material and the water. Note that, if the material of the filter is perfectly wettable, the contact angle is
31 equal to zero.

32 Two different ceramic filters were used in this work, namely a kaolinite ceramic filter (herein named KCF)
33 and an alumina ceramic filter (herein named ACF), which exhibit different mineralogical compositions and
34 porosity characteristics. The porosity characteristics of the two filters were measured by means of Mercury
35 Intrusion Porosimetry (MIP) and Nitrogen Adsorption (NA) tests, which detect voids of different sizes.
36 MIP tests determine the pore size distribution over the large void range from 7 nm up to 0.5 mm while NA
37 tests determine the pore size distribution over the small void range from 2 nm to 50 nm. The results from
38 the two tests must therefore be combined to achieve a full characterization of the pore-size distribution of
39 the material.

40 In MIP tests, the pore volume is determined from the amount of intruded mercury under a given pressure,
41 P while the corresponding pore diameter, d_{pore} is calculated from the Young-Laplace equation as:

$$42 \quad d_{pore} = \frac{4 \sigma_m \cos \theta_m}{P} \quad [2]$$

1 where, σ_m is the air-mercury surface tension (here assumed equal to 485 mN/m at 293 °K) and θ_m is the
2 contact angle between the filter material and the mercury (here assumed equal to 130°). In NA tests, the
3 pore size distribution is determined by measuring the adsorption and desorption of nitrogen on the pore
4 surface at different relative pressures and at a constant temperature of 77 °K, according to the method
5 proposed by Barret et al. (1951).

6 Figure 2 shows that the KCF and ACF exhibit markedly different porosity characteristics in terms of both
7 volume and sizes of voids. In particular, the KCF exhibits a polydisperse porosity distribution over a range
8 of relatively small diameters from 1 nm to 190 nm, with a peak at around 65 nm. Conversely, the ACF
9 exhibits a monodisperse distribution over a range of larger diameters (from 100 nm to 290 nm), with a peak
10 at around 230 nm. Each MIP and NA test was repeated twice, except for the MIP test on the ACF that was
11 repeated three times, to validate the correctness of the adopted laboratory procedures.

12 Equation 1 was used to estimate the theoretical AEV of both filters based on the measured porosity
13 characteristics. The largest pore size of the KCF is comprised between 165 nm and 220 nm, which
14 corresponds to a theoretical AEV between 1.3 MPa and 1.7 MPa according to Equation 1 (if the filter is
15 assumed to be perfectly wettable, i.e. $\theta_w = 0^\circ$). This calculation matches well the nominal AEV of the
16 ceramic filter, which is equal to 1.5 MPa (15 bar) according to technical documentation provided by the
17 supplier. For ease of interpretation, Figure 2 also shows the pore diameter calculated from Equation 1 in
18 correspondence of the nominal AEV of 1.5 MPa (15 bar), which matches well the upper limit of the MIP
19 curve. Conversely, the largest pore size of the ACF is comprised between 250 nm and 290 nm, which is
20 considerably larger than the largest pore size of the KCF and corresponds to a theoretical AEV between 1.0
21 MPa and 1.1 MPa according to Equation 1 (if the filter is assumed to be perfectly wettable, i.e. $\theta_w = 0^\circ$).
22 In this case, however, no nominal AEV was provided by the filter supplier, though air-breakthrough
23 experiments indicated that the AEV should be comprised between 0.7 and 1.0 MPa (7 and 10 bar
24 respectively). Once again, Figure 2 shows the pore diameter calculated from Equation 1 in correspondence
25 of an AEV of 1 MPa (10 bar), which matches well the upper limit of the MIP curve.

26 Table 1 summarizes the different characteristics of the two ceramic filters in terms of porosity, specific
27 density and bulk density. Inspection of Table 1 indicates that the ACF exhibits a significantly lower porosity
28 and a considerably higher specific density than the KCF, which results in a higher bulk density. These
29 characteristics are also consistent with the significantly higher levels of strength and hardness of the ACF
30 compared to the KCF.

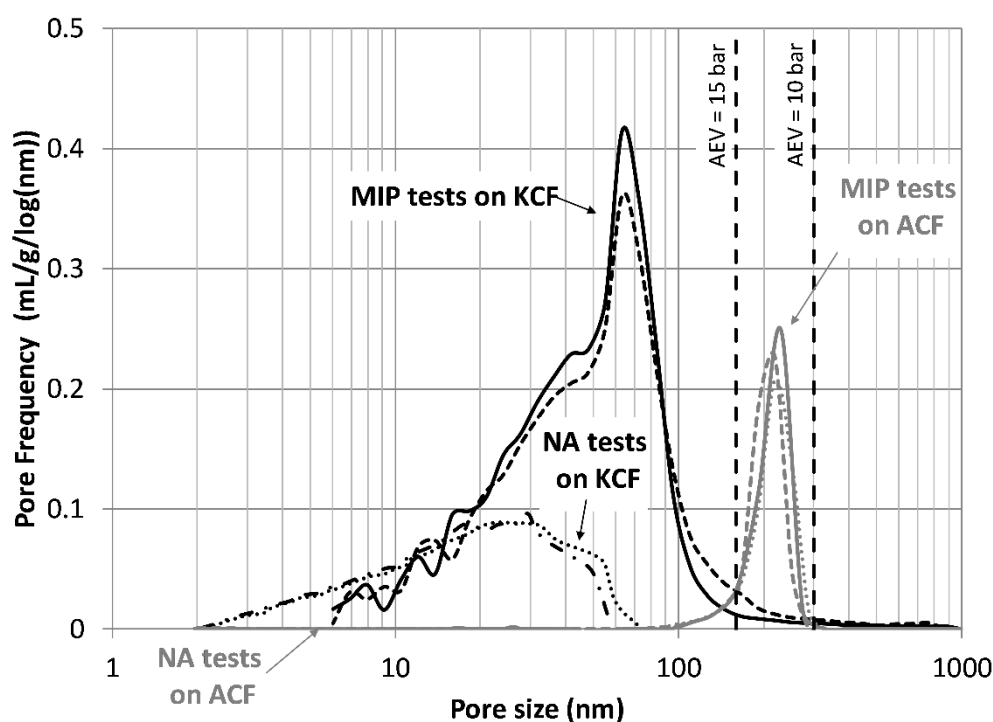


Figure 2. Pore size distribution of KCF and ACF measured by means of mercury intrusion porosimetry (MIP) and nitrogen adsorption (NA) tests.

Table 1. Ceramic filter properties.

	Pore size range nm	Largest pore nm	Porosity %	Specific density g/cm ³	Bulk density g/cm ³
KCF	2 - 220	165 - 220	33	2.02	1.35
ACF	95 - 290	250 - 290	13	3.10	2.70

3.2 Pressure transducers

The pressure transducer range should be equal to at least the AEV of the filter in order to exploit the full measuring potential of the HCT. The transducer must also be capable of recording both positive (compressive) and negative (tensile) water pressures to maximize sensor versatility but also to allow calibration. This is because calibration is normally performed in the positive pressure range and then extrapolated to the negative pressure range by assuming a symmetric response of the sensing diaphragm (Tarantino and Mongioví, 2002). A unique linear correlation is therefore assumed between transducer voltage and applied pressure, regardless of whether the sensing diaphragm is deforming towards the reservoir (if water pressure is negative) or away from the reservoir (if water pressure is positive). This assumption could be validated by imposing a positive pressure at the back of the sensing diaphragm (Tarantino and Mongioví, 2003), though this check is not commonly performed during HCT design.

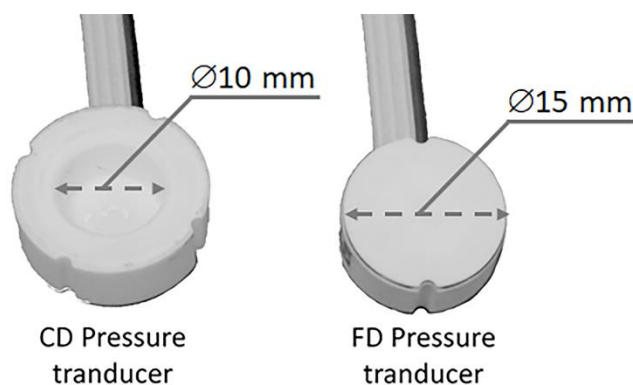
Two different pressure transducers were used in this work, namely a ceramic cavity diaphragm transducer (herein named CD) and a ceramic flush diaphragm transducer (herein named FD), which are both depicted

1 in Figure 3. These transducers are made of 96% pure alumina and their characteristics are summarized in
2 Table 2.

3 Both transducers have a full scale (FS) of 2000 kPa in the positive pressure range, though no information
4 is provided by the manufacturer about their ability to measure negative pressures. Technical documentation
5 also indicates a measurement accuracy equal to 0.5% of the full scale, which corresponds to an error margin
6 of ± 10 kPa. Therefore, a small full scale is preferable to maximize transducer accuracy, though a large full
7 scale is often necessary to apply high positive pressures that can dissolve all residual air nuclei during the
8 saturation of HCTs prior to use. A full scale of 2000 kPa has here been chosen as a compromise between
9 these two opposite requirements as it provides a good accuracy of ± 10 kPa while allowing the application
10 of a saturation pressure up to 4000 kPa. This very large value is admissible because the transducer
11 performance is compromised only when the applied pressure attains the overpressure limit of the device,
12 which is twice its full scale range. In this work, a saturation pressure of about 3000 kPa was chosen because
13 this value is two times greater than the AEV of the filter and is considered sufficient to achieve an adequate
14 dissolution of most residual air nuclei.

15 Another CD ceramic transducer, with a smaller measuring range of 500 kPa, was also used to achieve a
16 higher accuracy of ± 2.5 kPa at the price, however, of a lower pre-pressurisation which is likely to limit the
17 maximum sustainable water tension.

18



19

20 **Figure 3.** Ceramic cavity diaphragm (CD) pressure transducer (left) and ceramic flush diaphragm (FD)
21 pressure transducer (right).

22

23

Table 2. Pressure transducer characteristics.

Designation	Ceramic flush diaphragm	Ceramic cavity diaphragm
Short name	FD	CD
Sensor type	Piezoresistive	
Pressure reference	Relative to atmosphere	Relative to atmosphere
Pressure full scale range (FS) [kPa]	2000	500 / 2000
Accuracy [%FS]	0.5	

24

1 **3.3 Water reservoir**

2 The purpose of the water reservoir is to create a gap between the ceramic filter and the flexible diaphragm
3 of the pressure transducer, so that no contact occurs between these two components when the latter deflects
4 inwards during measurements of negative pore-water pressures. Two groups of HCT prototypes were
5 manufactured in this work to incorporate gaps of different sizes between the ceramic filter and the pressure
6 transducer. One group incorporates a small water reservoir, which is delimited by the flush diaphragm (FD)
7 transducer at the base and by the protective casing on the sides, thus resulting in a capacity of only 40 mm³.
8 Another group incorporates a large water reservoir defined by the shape of the cavity diaphragm (CD)
9 transducer which delimits both the base and the sides of the reservoir, thus resulting in a capacity of about
10 430 mm³. The details of the design of all HCT prototypes are discussed later in the paper.

11 The above transducer choices were aimed to investigate the effect of the water reservoir size on both the
12 measuring range and the long-term stability of measurements. The former effect is discussed in the present
13 paper while the latter effect is considered elsewhere (Mendes and Gallipoli, 2020).

14

15 **3.4 Protective casing**

16 The protective casing must be stiff enough to minimize any transfer of stresses to the transducer as this may
17 generate spurious measurements of pressure. The casing must also be chemically inert, i.e. it must not react
18 with water or any other compound commonly found in soils. This aspect is particularly important if the
19 water inside the reservoir is in direct contact with the inner surface of the casing. Finally, the casing should
20 exhibit a low thermal expansion/contraction coefficient to avoid the application of stresses to the sensing
21 unit as a consequence of temperature fluctuations, which are particularly frequent in field applications. The
22 utilization of epoxy glue may also contribute to the generation of internal stresses because of the different
23 thermal expansion coefficients of the pressure transducer and the epoxy that binds it (Toker et al., 2004).

24 Two types of protective casings were manufactured in the present work by using two different materials,
25 namely stainless steel 316 (herein named SS316) and 99% pure alumina ceramic (herein named Al). These
26 materials are very stiff and chemically inert, which satisfies the first two of the above three requirements.
27 As for thermal behaviour, however, both materials exhibit temperature-induced deformations, which
28 potentially poses a problem to the accuracy of measurements. Table 3 shows the main properties of the two
29 materials and indicates that alumina ceramic is preferable to stainless steel as it exhibits a smaller thermal
30 expansion coefficient, a higher specific heat and a higher stiffness. A higher specific heat means that the
31 material must exchange a larger amount of energy with the surrounding environment to attain a given
32 change of temperature. A higher specific heat therefore corresponds to a larger thermal inertia and
33 consequently to smaller temperature changes of the casing material, which is of course a desirable property.
34 Unfortunately, temperature-induced deformations cannot be eliminated and their effect on suction
35 measurements should be compensated based on calibration at different temperatures. This is particularly
36 important in field applications as, in this case, thermal fluctuations are more significant than in a controlled
37 laboratory environment.

38 The process of manufacture of the casing is also different depending on the chosen material, namely
39 stainless steel casings are machined out of solid rods while ceramic casings are casted to shape. In the
40 former case, fine geometric details such as threads, grooves or ridges can be included with relative ease and
41 mistakes can be generally rectified at a later stage. In the latter case, the casing geometry must be as
42 straightforward as possible because of the moulding process, which only allows for the inclusion of simple
43 details and makes virtually impossible any modification after casting.

44

45

46

1

Table 3. Main properties of casing materials.

		SS316	Al
Thermal coefficient of linear expansion	[10 ⁻⁶ K ⁻¹]	16	8
Thermal conductivity at 25°C	[W/(m.K)]	16	35
Specific heat	[J/(kg.K)]	500	880
Stiffness (Young modulus)	GPa	200	360

2

3 3.5 HCT prototype designs

4 Table 4 shows the five HCT designs developed in the present work. Two of these designs were implemented
5 in two different versions, using different ceramic filters and pressure transducers, which gives a total of
6 seven HCT prototypes. All prototypes have a cylindrical shape with a length between 35 and 60 mm and a
7 diameter of about 26 mm. The prototypes are named according to the format VVV – WW(XXXX) –
8 YYYYY [Z], which describes the different design components. In particular, VVV indicates the ceramic
9 filter (KCF or ACF), WW indicates the pressure transducer (FD or CD), XXXX indicates the measuring
10 range of the transducer in kPa (500 or 2000), YYYYY indicates the casing material (SS316 or Al) and,
11 finally, Z indicates a design variant (1 or 2).

12 The first three prototypes in the first two rows of Table 4, i.e. KCF – FD(2000) – SS316 [1], ACF –
13 FD(2000) – SS316 and KCF – FD(2000) – Al, were built around a flush diaphragm pressure transducer. In
14 these three prototypes, the water reservoir was created via a special design of the casing, which incorporates
15 a recess that is deeper than the height of the pressure transducer. The transducer fits inside the recess while
16 the ceramic filter sits on the external edge of the recess, thus creating a small cylindrical gap between the
17 transducer and the filter. This gap has a depth of 0.2 mm and a diameter of 16 mm, which results in a
18 volume of about 40 mm³. The sides of both the transducer and the ceramic filter were sealed against the
19 inner surface of the casing by means of an epoxy resin. The inner surface of the casing therefore delimits
20 the perimeter of the reservoir.

21 The fourth prototype in the third row of Table 4, i.e. KCF – FD(2000) – SS316 [2], was built around a flush
22 diaphragm pressure transducer likewise the previous three prototypes. The water reservoir was again
23 created through a particular design of the casing, which includes a thin protruding lip that separates the
24 ceramic filter from the transducer. The thickness of this lip creates a cylindrical gap between the filter and
25 the transducer with a depth of 0.5 mm and a diameter of 10 mm, which results in a reservoir volume of
26 about 40 mm³. A threaded adaptor was screwed on the back of the casing to push the pressure transducer
27 against the protruding lip, thus securing it in place. The purpose of this design was to prevent any potential
28 movement of the transducer when subjected to both negative (tensile) water pressures during measurements
29 and positive (compressive) water pressures during saturation and calibration. Like the previous prototypes,
30 the transducer and the ceramic filter were sealed against the inner sides of the casing by means of an epoxy
31 resin.

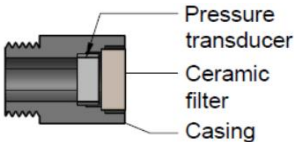
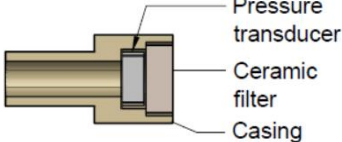
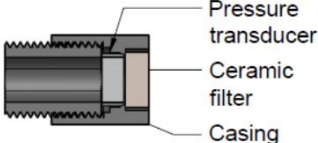
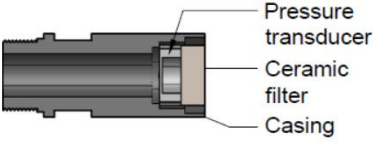
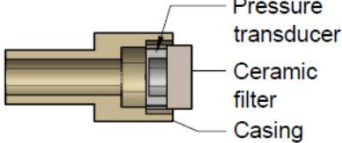
32 The last three prototypes in the fourth and fifth rows of Table 4, i.e. KCF – CD(2000) – SS316, KCF –
33 CD(2000) – Al and KCF – CD(500) – Al, were built around a cavity diaphragm pressure transducer. In
34 these prototypes, the ceramic filter was directly sealed against the rim of the hollow transducer, whose inner
35 cavity therefore delimited the base and the perimeter of the reservoir. The transducer cavity has a diameter
36 of 10 mm and a depth of 5.5 mm resulting in a reservoir volume of about 430 mm³, which is more than ten
37 times larger compared to the previous four prototypes. The cavity diaphragm transducer and the ceramic
38 filter were glued together by means of an epoxy resin before being slotted as a single piece inside the casing
39 where they were again sealed by means of an epoxy resin. In this case, unlike previous prototypes, the
40 casing is not in direct contact with the water inside the reservoir. Note that the two prototypes KCF –

1 CD(2000) – AI and KCF – CD(500) – AI have identical appearances in Table 4 as they differ solely for the
 2 transducer full scale range, which is equal to 2000 kPa in the former case and 500 kPa in the latter case.

3

4

Table 4. Designs of HCT prototypes.

 <p>Pressure transducer Ceramic filter Casing</p>	<p>Name: KCF – FD(2000) – SS316 [1] and ACF – FD(2000) – SS316</p> <p>Size: 35 mm x \varnothing26 mm</p> <p>Ceramic filter: KCF or ACF</p> <p>Water reservoir size: 40mm³ (0.2 mm x \varnothing16 mm)</p> <p>Pressure transducer: 2000kPa ceramic flush diaphragm</p> <p>Casing material: Stainless steel SS316</p> <p>Special feature: Water reservoir included in the casing design</p>
 <p>Pressure transducer Ceramic filter Casing</p>	<p>Name: KCF – FD(2000) – AI</p> <p>Size: 50 mm x \varnothing26 mm</p> <p>Ceramic filter: KCF</p> <p>Water reservoir size: 40mm³ (0.2 mm x \varnothing16 mm)</p> <p>Pressure transducer: 2000kPa ceramic flush diaphragm</p> <p>Casing material: Alumina ceramic</p> <p>Special feature: Water reservoir included in the casing design</p>
 <p>Pressure transducer Ceramic filter Casing</p>	<p>Name: KCF – FD(2000) – SS316 [2]</p> <p>Size: 45 mm x \varnothing26 mm</p> <p>Ceramic filter: KCF</p> <p>Water reservoir size: 40mm³ (0.5 mm x \varnothing10 mm)</p> <p>Pressure transducer: 2000kPa ceramic flush diaphragm</p> <p>Casing material: Stainless steel SS316</p> <p>Special features: small lip in the casing design that separates ceramic filter and pressure transducer; use of a thread adaptor to secure the pressure transducer in place</p>
 <p>Pressure transducer Ceramic filter Casing</p>	<p>Name: KCF – CD(2000) – SS316</p> <p>Size: 60 mm x \varnothing26 mm</p> <p>Ceramic filter: KCF</p> <p>Water reservoir size: 430mm³ (5.5 mm x \varnothing10 mm)</p> <p>Pressure transducer: 2000kPa ceramic cavity diaphragm</p> <p>Casing material: Stainless steel SS316</p> <p>Special feature: cavity of the pressure transducer used as water reservoir</p>
 <p>Pressure transducer Ceramic filter Casing</p>	<p>Name: KCF – CD(2000) – AI and KCF – CD(500) – AI</p> <p>Size: 55 mm x \varnothing26 mm</p> <p>Ceramic filter: KCF</p> <p>Water reservoir size: 430mm³ (5.5 mm x \varnothing10 mm)</p> <p>Pressure transducer: 500kPa and 2000kPa ceramic cavity diaphragm</p> <p>Casing material: Alumina ceramic</p> <p>Special feature: cavity of the pressure transducer used as water reservoir</p>

5

4 Performance of HCT prototypes

The performance of the previous HCT prototypes was then compared in terms of the time required for saturation, the calibration accuracy in the positive pressure range and the maximum sustainable water tension.

4.1 Saturation and calibration of HCT prototypes

An adequate water saturation of both porous filter and reservoir is crucial for the good performance of HCTs during suction measurements. Two different saturation procedures were adopted in this work depending on whether the HCT was dry or “quasi-saturated” with only few small gas cavities in the porous filter and reservoir. The former saturation procedure is termed “first saturation” and is typically applied to a newly built HCT that is completely dry. The latter saturation procedure is instead termed “re-saturation” and is typically applied to an initially saturated HCT that has experienced cavitation during suction measurement leading to the formation of few small gas cavities inside the filter and reservoir. The gas cavities that have formed during cavitation must be eliminated to restore the sensor ability to record water tensions.

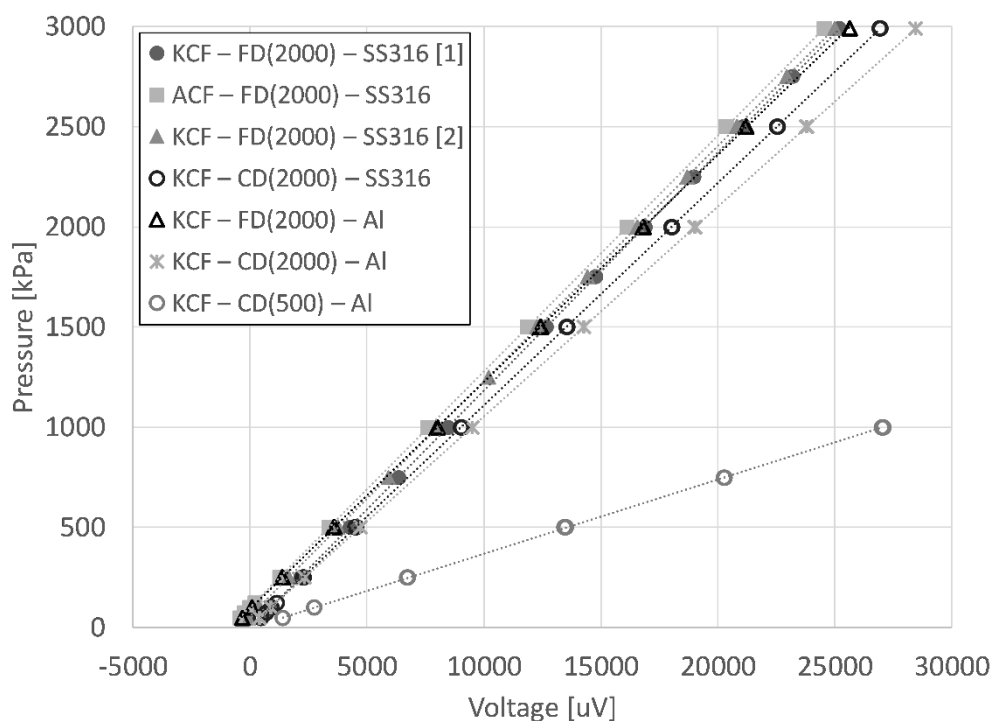
Marinho and Chandler (1994) suggested that the first saturation of HCTs should include the application of high vacuum followed by water flooding and pressurization. The application of high vacuum is necessary to minimize the amount of residual air inside the porous filter and reservoir prior to flooding while the subsequent pressurization helps dissolve any remaining gas cavities. Consistent with the above recommendations, a two stages procedure was adopted in this work for the first saturation of all HCTs. In the first stage, the filter was exposed to the vacuum created by a Pfeiffer DUO 11 two stage rotary vane vacuum pump delivering an ultimate absolute pressure of $3 \cdot 10^{-4}$ kPa. During exposure to vacuum, the HCT readings were continuously monitored and stabilized after about 15 min. Once stabilization was achieved, the vacuum was maintained for a further hour to evacuate most of the entrapped air. The de-aired water line was then opened and the water, under atmospheric pressure, rapidly flooded the porous filter and reservoir. In the second stage, the water was compressed inside the HCT by means of a VJTech automatic pressure/volume controller capable of applying a maximum pressure of 2990 kPa. A compressive pressure of 2990 kPa was applied to all HCT prototypes except prototype KCF – CD(500) – Al, which was instead subjected to a lower pressure of 1000 kPa to avoid damaging the transducer. This was necessary because prototype KCF – CD(500) – Al incorporates a transducer with a measuring range of 500 kPa instead of 2000 kPa like all other cases. A pressurization time between 12 and 24 hours was found to be sufficient to saturate the HCT prototypes with the smaller water reservoir built around a flush diaphragm transducer, namely KCF – FD(2000) – SS316 [1], KCF – FD(2000) – SS316 [2], ACF – FD(2000) – SS316 and KCF – FD(2000) – Al. A longer pressurization time up to 96hrs was instead necessary to saturate the HCT prototypes with the larger water reservoir built around a cavity pressure transducer, namely KCF – CD(2000) – SS316, KCF – CD(2000) – Al and KCF – CD(500) – Al.

Instead, the re-saturation procedure involved a simple pressurization to either 2990 or 1000 kPa, depending on the measuring range of the pressure transducer, without any previous application of vacuum. This pressurization stage varied from minutes to hours depending on the time the HCT was left exposed to the atmosphere after cavitation. This procedure was found to be enough for restoring the ability of all HCTs to record negative pore-water pressures.

Calibration of all HCTs took place in the positive (compressive) pressure range and was subsequently linearly extrapolated to the negative (tensile) pressure range as discussed by Tarantino and Mongiovi (2003). A positive pressure cycle of 2990 kPa→50 kPa→2990 kPa was imposed to the HCT prototypes incorporating the transducers with a measuring range of 2000 kPa, namely KCF – FD(2000) – SS316 [1], KCF – FD(2000) – SS316 [2], ACF – FD(2000) – SS316, KCF – FD(2000) – Al, KCF – CD(2000) – SS316 and KCF – CD(2000) – Al. A smaller pressure cycle of 1000 kPa→50 kPa→1000 kPa was instead imposed to the single HCT prototype incorporating a pressure transducer with a measuring range of 500 kPa, namely

1 KCF – CD(500) – Al. The maximum pressure applied during calibration was higher than the full scale
 2 range but smaller than the overload limit to avoid damaging the transducer. The application of such extreme
 3 pressure levels was helpful to explore the linearity of the transducer response even beyond the full scale
 4 range. The results of the different calibrations are summarized in Figure 4, which shows the relationship
 5 between pressure and voltage for all HCT prototypes. Inspection of Figure 4 indicates that, regardless of
 6 reservoir size, ceramic filter and transducer type, all HCT prototypes exhibit a linear response over the
 7 applied pressure range with a negligible hysteresis of 0.04%. This result confirms that the applied pressure
 8 can be safely pushed beyond the full scale range, provided that the overpressure limit is not exceeded, thus
 9 achieving a reasonable compromise between accuracy and pre-pressurisation as discussed in Section 3.2.

10



11

12

Figure 4. Calibration curves of HCT prototypes.

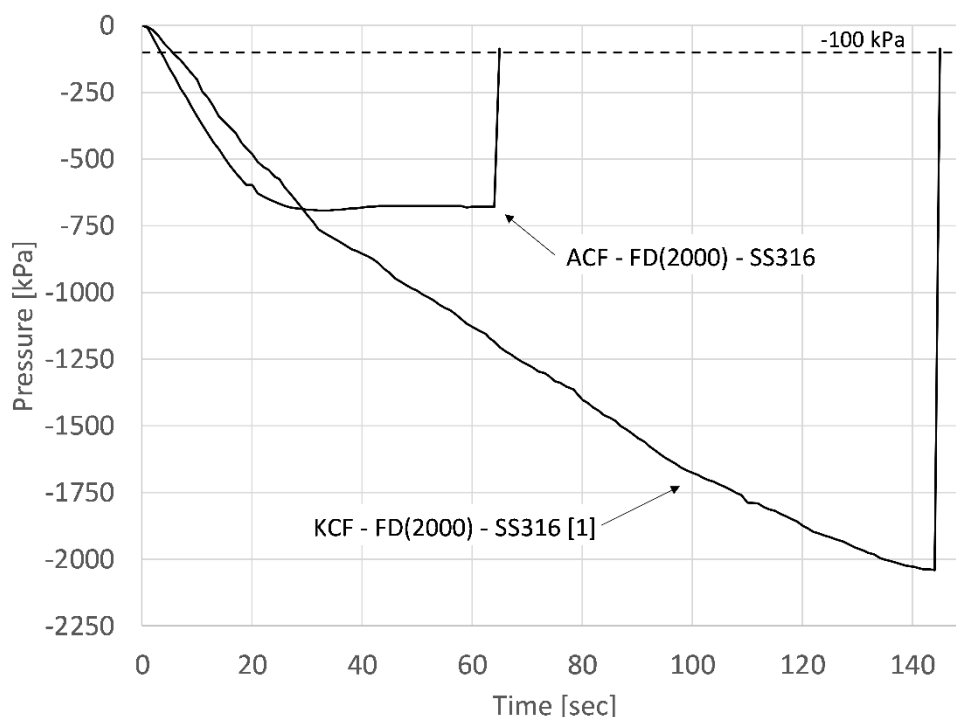
13

14 **4.2 Maximum sustainable water tension of HCT prototypes**

15 All HCT prototypes were subjected to evaporation tests to determine their respective maximum sustainable
 16 water tensions or, in other words, their respective measuring ranges. During these tests, the HCT prototypes
 17 were exposed to the atmosphere, thus allowing the progressive depletion of water from the menisci at the
 18 outer face of the filter. This evaporation generates an increasingly larger water tension inside the saturated
 19 filter, which propagates almost instantaneously to the reservoir causing the inward deflection of the
 20 transducer diaphragm. The HCT therefore reads increasingly larger water tensions (i.e. negative water
 21 pressures) until a sudden breakdown of measurements occurs leading to an instantaneous rise of pressure
 22 to about -100 kPa, which is close to the water vapour gauge pressure. This breakdown of measurements
 23 corresponds to the expansion of small gas cavities inside the water reservoir and is commonly termed
 24 “cavitation”. The lowest (negative) water pressure recorded immediately before cavitation is here taken as
 25 the maximum sustainable water tension.

26 Prototypes KCF – FD(2000) – SS316 [1] and ACF – FD(2000) – SS316 have identical pressure transducers,
 27 reservoir sizes, and protective casings but different ceramic filters. By comparing the results from their

1 respective evaporation tests, it is therefore possible to evaluate the effects of the KCF (whose nominal AEV
 2 is 1.5 MPa) and the ACF (whose estimated AEV is 1.0 MPa) on the maximum sustainable water tension.
 3 Figure 5 shows the results from a typical evaporation test for each of these two prototypes and indicates
 4 that the prototype incorporating the KCF attains a lower water pressure before cavitation (about -2000 kPa)
 5 compared to the prototype incorporating the ACF (about -700 kPa). This is consistent with the data shown
 6 in Figure 2 and Table 1, which indicate that the KCF exhibits a smaller pore size and, hence, a larger AEV
 7 than the ACF. The prototype incorporating the KCF can therefore sustain higher water tensions compared
 8 to the prototype incorporating the ACF. The use of the ACF may however still be preferable in harsh field
 9 conditions, where robustness is important, because of its higher density and hardness (Table 2).



10
 11 **Figure 5.** Typical evaporation tests on identical prototypes incorporating different ceramic filters (ACF –
 12 FD(2000) – SS316 and KCF – FD(2000) – SS316 [1]).

13
 14 Given the larger AEV of the KCF compared to the ACF, six out of the seven prototypes manufactured in
 15 the present work incorporated the KCF. Figure 6 shows the results from one typical evaporation test for
 16 each of these six prototypes while Table 5 presents the minimum water pressures registered just before
 17 cavitation during five distinct evaporation tests for each prototype. Inspection of Figure 6 and Table 5
 18 indicates that, regardless of reservoir size, pressure transducer and protective casing, the ultimate water
 19 pressure recorded before cavitation is always lower than -1500 kPa.

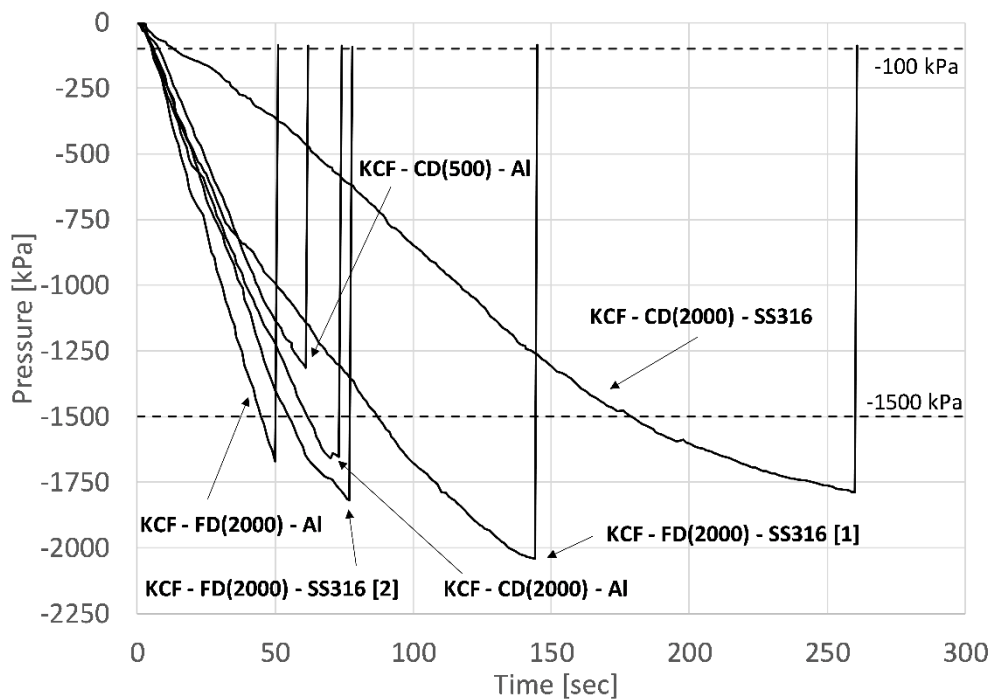
20 The only exception is given by prototype KCF – CD(500) – Al, which incorporates a pressure transducer
 21 with a full scale range of 500 kPa instead of 2000 kPa. As previously discussed, the smaller full scale range
 22 required the application of a lower positive pressure (1000 kPa) during saturation and calibration of this
 23 prototype to prevent damaging the transducer. This might have hampered the dissolution of air cavities
 24 inside the ceramic filter and water reservoir, which is the reason why the maximum tension is lower
 25 compared to the other prototypes. It is however worth highlighting that, despite the low pre-pressurisation,
 26 prototype KCF – CD(500) – Al was still capable of measuring significant water tensions, up to about -1300
 27 kPa, which is even larger than the overload limit of the transducer (1000 kPa). It was later checked that
 28 calibration had not changed despite the relatively large value of the maximum measured tension. Therefore,

1 if high accuracy is required especially in the low suction range, a transducer with a smaller full scale can
2 possibly be employed.

3 Figure 6 shows that the evaporation rate is approximately similar for all prototypes and that the time to
4 cavitation ranges between 50 and 140 seconds. The only exception to this behaviour is provided by
5 prototype KCF – CD(2000) – SS316, which exhibits a significantly slower evaporation rate taking about
6 260 seconds to reach cavitation. The slower response of this prototype was initially attributed to its
7 relatively large reservoir size but this hypothesis was subsequently disproved by the tests on prototype KCF
8 – CD(2000) – Al, which has an identical reservoir size but exhibits a faster response. Prototypes KCF –
9 CD(2000) – SS316 and KCF – CD(2000) – Al are virtually identical with the only difference being the
10 material of the casing which should, however, have no effect as the casing is not in direct contact with the
11 water inside the reservoir (Table 4).

12 It was later speculated that the different behaviour of prototypes KCF – CD(2000) – Al and KCF –
13 CD(2000) – SS316 might have been caused by the different epoxy resins used to assemble the two
14 prototypes. In particular, an epoxy resin for ceramics and metals was used to assemble the KCF – CD(2000)
15 – Al prototype while an epoxy resin for casting/potting was employed to assemble the KCF – CD(2000) –
16 SS316 prototype. Note, however, that the stiffnesses of the two resins are very similar, i.e. 2400 MPa in the
17 former case compared to 2900 MPa in the latter case, which suggests that an explanation should rather be
18 found in the different chemical properties of the resins, though this hypothesis requires further investigation.

19



20

21 **Figure 6.** Typical evaporation tests on different prototypes incorporating identical ceramic filters (KCF).

22

23

24

25

26

1 **Table 5.** Water tensions recorded during multiple tests on different HCT prototypes just before cavitation.

HCT prototype	KCF	KCF	KCF	KCF	KCF	KCF
	FD(2000) SS316 [1]	FD(2000) Al	FD(2000) SS316 [2]	CD(2000) SS316	CD(2000) Al	CD(500) Al
Recorded cavitation pressure [kPa]	-1563	-1582	-1676	-1641	-1605	-1256
	-1642	-1603	-1677	-1718	-1646	-1284
	-1669	-1623	-1699	-1735	-1666	-1302
	-1896	-1788	-1735	-1774	-1754	-1305
	-2041	-1965	-1819	-1976	-1932	-1314

2 **5 Conclusions**

3 This article has discussed the effect of sensor design on the saturation, calibration and maximum measurable
4 water tension of High Capacity Tensiometers (HCTs). In particular, the study has compared the
5 performance of seven distinct HCT incorporating different pressure transducers, porous filters, water
6 reservoir sizes, protective casings and epoxy resins.

7 Among all design variables, the air entry value (AEV) of the porous filter appears to have the strongest
8 influence on the maximum water tension recorded by the HCTs and, hence, on their measuring range.
9 Evaporation tests showed that the maximum water tension, measured just before cavitation, was larger
10 when the AEV of the filter was bigger, thus confirming past evidence that a properly saturated HCT is
11 generally capable of measuring a maximum tension close to the AEV of the filter. In particular, the HCT
12 prototypes incorporating a kaolin ceramic filter with an AEV of 15 bar measured a maximum water tension
13 between -1800 kPa and -2000 kPa while the HCT prototypes incorporating an alumina ceramic filter with
14 an AEV between 7 and 10 bar measured a maximum water tension between -700 kPa and -800 kPa.
15 Moreover, the analysis of results from porosimetry tests on both ceramic filters confirmed that the AEV is
16 inversely related to the size of the largest pore in the filter.

17 Contrary to common belief, the size of the water reservoir does not seem to affect the response time of
18 HCTs during evaporation tests, nor does it influences the maximum water tension recorded before
19 cavitation. This may be because cavitation is triggered by gas nuclei that are either located in the porous
20 filter (Mendes and Buzzi, 2013) or on the reservoir surface which, unlike the reservoir volume, did not
21 change significantly between prototypes. It is however still unclear whether the reservoir size influences
22 the long-term performance of HCTs and the stability of measurements over time. This is an important aspect
23 to consider for field monitoring applications and is the object of a companion paper (Mendes and Gallipoli,
24 2020). Special consideration should also be given to the process of fabricating HCTs and to the type of
25 epoxy resin used to assemble the sensor components, especially if the resin is in direct contact with the
26 water inside the sensor.

27 Consistent with past studies, this work indicates that the procedures for the first saturation and re-saturation
28 of HCTs can have a significant influence on the measuring performance of the sensors. In particular, the
29 application of a large positive pressure may considerably increase the maximum sustainable water tension.
30 This is evident by comparing the results from the evaporation tests performed on two similar prototypes
31 subjected to different saturation pressures of 1000 kPa and 2990 kPa, respectively. The maximum water
32 tension recorded by the former prototype was about 25% smaller than the maximum tension recorded by
33 the latter prototype.

1 Acknowledgements

2 The financial contribution of the European Commission to this research through the Marie Curie Industry-
3 Academia Partnership and Pathways Network MAGIC (Monitoring systems to Assess Geotechnical
4 Infrastructure subjected to Climatic hazards) – PIAPP-GA-2012-324426 – is gratefully acknowledged.

5 References

- 6 Bagheri, M., Rezaia M. and Mousavi Nezhad M., 2018. Cavitation in high-capacity tensiometers: effect
7 of water reservoir surface roughness. *Geotechnical Research* 5(2): 81–95.
- 8 Barrett, E.P., Joyner, L.G., Halenda, P.P., 1951. The determination of pore volume and area distributions
9 in porous substances. I. Computations from nitrogen isotherms *J. Am. Chem. Soc.* 73: 373–380.
- 10 Delage, P., Romero, E. and Tarantino, A. 2008. Keynote Lecture: Recent developments in the techniques
11 of controlling and measuring suction. *Proc. 1st European Conference on Unsaturated Soils, 2-4th July*
12 2008, Durham, UK: 33-52.
- 13 Caruso, A., Tarantino, A., 2004. A shearbox for testing unsaturated soils from medium to high degrees of
14 saturation. *Geotechnique* 54(4):281-284.
- 15 Cui, Y.J., Tang, A., Mantho, A., De Laure, E., 2008. Monitoring field soil suction using a miniature
16 tensiometer. *Geotechnical Testing Journal* 31(1): 95-100.
- 17 Cunningham, M. R., Ridley, A. M., Dineen, K. and Burland, J. B. 2003. The mechanical behaviour of a
18 reconstituted unsaturated silty clay. *Géotechnique*, 53: 183-194.
- 19 Giesche, H., 2006. Mercury porosimetry: a general (practical) overview. *Part. Part. Syst. Charact.*, 23:9-19.
- 20 Guan, Y., Fredlund, D.G., 1997. Use of the tensile strength of water for the direct measurement of high soil
21 suction. *Canadian Geotechnical Journal*, 34(4): 604-614.
- 22 Le, T.T., Cui, Y.J. and Muñoz, J., Delage, P., Tang, A.M. and Li, X.L., (2011). Studying the stress-suction
23 coupling in soils using an oedometer equipped with a high capacity tensiometer. *Frontiers of*
24 *Architecture and Civil Engineering in China*. 5. 160-170. 10.1007/s11709-011-0106-x.
- 25 Lourenço, S.D.N., Gallipoli, D., Toll, D.G., Augarde, C., Evans, F., Medero, G.M., 2008. Calibration of a
26 high-suction Tensiometer. *Géotechnique* 58(8): 659-668.
- 27 Marinho, F.A.M., Chandler, R.J., 1994. Discussion on A new instrument for the measurement of soil
28 moisture suction. *Géotechnique* 44(3): 551-556.
- 29 Marinho, F.A.M., and de Sousa Pinto, C. (1997). Soil suction measurement using a tensiometer.
30 *Symposium on Recent Development in Soil and Pavement Mechanics - Rio de Janeiro, June.* pp. 249-
31 254.
- 32 Marinho F.A.M., Take A. and Tarantino A. 2008. Tensiometric and axis translation techniques for suction
33 measurement. *Geotechnical and Geological Engineering*, 26(6): 615-631.
- 34 Meilani, I., Rahardjo, H., Leong, E.C., Fredlund, D.G., 2002. Mini suction probe for matric suction
35 measurements. *Canadian Geotechnical Journal* 39: 1427-1432.
- 36 Mendes, J., Buzzi, O., 2013. New insight into cavitation mechanisms in high-capacity tensiometers based
37 on high-speed photography. *Canadian Geotechnical Journal* 50(5): 550-556.
- 38 Mendes, J., Buzzi, O., 2014. Performance of the University of Newcastle high capacity tensiometers. *Proc.*
39 *UNSAT 2014, Unsaturated Soils: Research and Applications, Sydney Australia:* 1611-1616.

- 1 Mendes, J., Gallipoli, D., 2020. Comparison of high capacity tensiometer designs for the long-term
2 measurements of soil suction. *Physics and Chemistry of the Earth*, 115: 102831.
3 <https://doi.org/10.1016/j.pce.2019.102831>
- 4 Mendes, J., Gallipoli, D., Plantier, F., Gregoire, D., 2015. Filtres de ceramique pour tensiometres a haute
5 capacite. In *Proceedings Rencontres Universitaires de Genie Civil, Bayonne, France*.
- 6 Mendes, J., Toll, D.G., 2016. Influence of initial water content on the mechanical behaviour of unsaturated
7 sandy clay soil. *Int J Geomech* 16(6):D4016005
- 8 Mendes, J., Toll, D.G., Augarde, C.E., Gallipoli, D., 2008. A system for field measurement of suction
9 using high capacity tensiometers. In *Unsaturated Soils: Advances in Geo-Engineering, Proceedings*
10 *1st European Conference on Unsaturated Soils, Durham, United Kingdom*, 219-225.
- 11 Ridley, A.M., Burland, J.B., 1993. A new instrument for the measurement of soil moisture suction.
12 *Géotechnique* 43(2): 321-324.
- 13 Take, W.A., Bolton, M.D., 2003. Tensiometer saturation and the reliable measurement of soil suction.
14 *Géotechnique* 54(3): 159-172.
- 15 Tarantino, A., Mongiovì, L., 2001. Experimental procedures and cavitation mechanisms in tensiometer
16 measurements. *Geotech. Geol. Engng* 19, No. 3, 191–210.
- 17 Tarantino, A., Mongiovì, L., 2002. Design and construction of a tensiometer for direct measurement of
18 matric suction. In *Proceedings 3rd International Conference on Unsaturated soils, Recife, Brazil*, 1:
19 319-324.
- 20 Tarantino, A. and Mongiovì, L. (2003). Calibration of tensiometer for direct measurement of matric suction.
21 *Géotechnique*, Technical Note, 53, No.1, 137-141.
- 22 Tarantino A. and De Col E. 2008. Compaction behaviour of clay. *Géotechnique* 58(3): 199–213.
- 23 Toll D.G., Lourenço S.D.N. Mendes J., Gallipoli D., Evans F.D., Augarde C.E., Cui Y.J., Tang A.M., Rojas
24 J.C., Pagano, L. Mancuso C., Zingariello C. and Tarantino A. 2011. Soil suction monitoring for
25 landslides and slopes. *Quarterly Journal of Engineering Geology and Hydrogeology*, 44, 1–13. DOI
26 10.1144/1470-9236/09-010
- 27 Toker, N. K., Germaine, J. T., Sjoblom, K. J. ve Culligan, P. J. (2004). "A new technique for rapid
28 measurement of continuous soil moisture characteristic curves", *Géotechnique*, Vol.54, No.3, p.179-
29 186.
- 30 Wijaya, Martin and Leong, E. (2016). Performance of high-capacity tensiometer in constant water content
31 oedometer test. *International Journal of Geo-Engineering*. 7. 13. 10.1186/s40703-016-0027-6.
- 32 Zheng, Q., Durben, D.J., Wolf, G.H., Angell, C.A., 1991. Liquids at large negative pressure: water at the
33 homogeneous nucleation limit. *Science*: 254: 829-832.
- 34

List of tables:

Table 1. Ceramic filter properties.

	Pore size range nm	Largest pore nm	Porosity %	Specific density g/cm ³	Bulk density g/cm ³
KCF	2 - 220	165 - 220	33	2.02	1.35
ACF	95 - 290	250 - 290	13	3.10	2.70

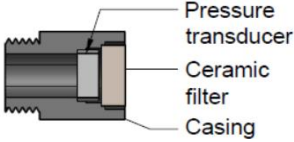
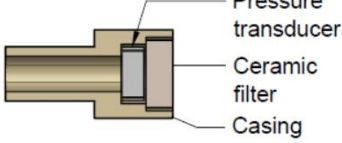
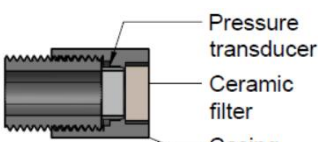
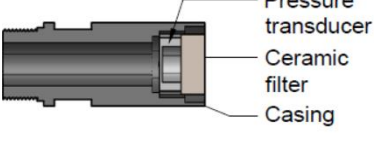
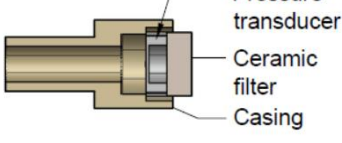
Table 2 – Pressure transducer characteristics.

Designation	Ceramic flush diaphragm	Ceramic cavity diaphragm
Short name	FD	CD
Sensor type	Piezoresistive	
Pressure reference	Relative to atmosphere	Relative to atmosphere
Pressure full scale range (FS) [kPa]	2000	500 / 2000
Accuracy [%FS]	0.5	

Table 3. Main properties of casing materials.

		SS316	Al
Thermal coefficient of linear expansion	[10 ⁻⁶ K ⁻¹]	16	8
Thermal conductivity at 25°C	[W/(m.K)]	16	35
Specific heat	[J/(kg.K)]	500	880
Stiffness (Young modulus)	GPa	200	360

1 **Table 4.** Designs of HCT prototypes.

 <p>Pressure transducer Ceramic filter Casing</p>	<p>Name: KCF – FD(2000) – SS316 [1] and ACF – FD(2000) – SS316 Size: 35 mm x \varnothing26 mm Ceramic filter: KCF or ACF Water reservoir size: 40mm³ (0.2 mm x \varnothing16 mm) Pressure transducer: 2000kPa ceramic flush diaphragm Casing material: Stainless steel SS316 Special feature: Water reservoir included in the casing design</p>
 <p>Pressure transducer Ceramic filter Casing</p>	<p>Name: KCF – FD(2000) – Al Size: 50 mm x \varnothing26 mm Ceramic filter: KCF Water reservoir size: 40mm³ (0.2 mm x \varnothing16 mm) Pressure transducer: 2000kPa ceramic flush diaphragm Casing material: Alumina ceramic Special feature: Water reservoir included in the casing design</p>
 <p>Pressure transducer Ceramic filter Casing</p>	<p>Name: KCF – FD(2000) – SS316 [2] Size: 45 mm x \varnothing26 mm Ceramic filter: KCF Water reservoir size: 40mm³ (0.5 mm x \varnothing10 mm) Pressure transducer: 2000kPa ceramic flush diaphragm Casing material: Stainless steel SS316 Special features: small lip in the casing design that separates ceramic filter and pressure transducer; use of a thread adaptor to secure the pressure transducer in place</p>
 <p>Pressure transducer Ceramic filter Casing</p>	<p>Name: KCF – CD(2000) – SS316 Size: 60 mm x \varnothing26 mm Ceramic filter: KCF Water reservoir size: 430mm³ (5.5 mm x \varnothing10 mm) Pressure transducer: 2000kPa ceramic cavity diaphragm Casing material: Stainless steel SS316 Special feature: cavity of the pressure transducer used as water reservoir</p>
 <p>Pressure transducer Ceramic filter Casing</p>	<p>Name: KCF – CD(2000) – Al and KCF – CD(500) – Al Size: 55 mm x \varnothing26 mm Ceramic filter: KCF Water reservoir size: 430mm³ (5.5 mm x \varnothing10 mm) Pressure transducer: 500kPa and 2000kPa ceramic cavity diaphragm Casing material: Alumina ceramic Special feature: cavity of the pressure transducer used as water reservoir</p>

2
3
4

1 **Table 5.** Water tensions recorded by different HCT prototypes just before cavitation.

HCT prototype	KCF FD(2000) SS316 [1]	KCF FD(2000) Al	KCF FD(2000) SS316 [2]	KCF CD(2000) SS316	KCF CD(2000) Al	KCF CD(500) Al
Recorded cavitation pressure [kPa]	-1563	-1582	-1676	-1641	-1605	-1256
	-1642	-1603	-1677	-1718	-1646	-1284
	-1669	-1623	-1699	-1735	-1666	-1302
	-1896	-1788	-1735	-1774	-1754	-1305
	-2041	-1965	-1819	-1976	-1932	-1314

2